



Estimation of Loads Acting on Flaps of the Su-22 Aircraft for Fatigue Tests

Grzegorz KOWALECZKO^{1*}, Andrzej LESKI², Wojciech ZIELIŃSKI²

¹ Polish Air Force Academy,
35 Dywizjonu 303 Street, 08-521 Dęblin, Poland

² Institute of Air Force Engineering
6 Księcia Bolesława Street, 01-494 Warsaw, Poland

* Corresponding author's e-mail address: g.kowaleczko@upcpoczta.pl

Received by the editorial staff on 27 July 2015.

The reviewed and verified version was received on 4 November 2015.

DOI 10.5604/01.3001.0009.2985

Abstract. The paper presents the results of the calculation of forces acting on the flaps of the Su-22 aircraft during take-off and landing. Four different analytic and experimental calculation methods were used to increase the reliability of the obtained results. The results will be the basis for performance of fatigue testing of the flaps which are structural components of the aircraft wings. The tests will be performed as part of a wider research program aimed at the extension of the Su-22 aircraft service life.

Keywords: mechanics, aircraft fatigue tests, aerodynamic loads, aircraft flaps

1. INTRODUCTION

Determination of in-flight loads acting on aircraft structural components is a task which new aircraft design engineering teams must carry out frequently.

This determination is based on analytical or computer calculations and is followed by experimental verification [4]. Computer-aided methods have been developed lately, facilitating precise modelling of aircraft structure airflow. The increased computing capacity of computers has made the calculations increasingly accurate and faster to complete. However, the related methods are still time-consuming, expensive and of limited availability due to the purchase costs of software, the necessary high computing capacity of computers, and the necessity of modelling the investigated structures in a computer-based environment.

Analytical methods remain as a valid alternative to computer-based methods. Analytical methods facilitate fast estimation of load values with relatively straightforward calculations. Most often, the cornerstone of analytical methods are characteristics determined by experimental testing. This facilitates a fast knowledge transfer to similar research cases. Although with a number of constraints, analytical methods facilitate evaluation of the magnitude of the loads acting on airframe structural components with theoretical and experimental relationships. The analytical methods have proven their feasibility through decades of application at various design engineering and research centres. They may still remain useful where a relatively fast and reliable determination is required to identify the loads on aircraft structures which have been operated for many years, especially where the comprehensive design documentation of the aircraft is missing. In this case, fragmentary data must be relied upon and complemented by direct measurements of the aircraft structure. This is the case with the Su-22 aircraft (Fig. 1). The Polish Air Forces have decided to extend the service life of the machine, which necessitates testing to prove the durability of the aircraft structure. The objective of the tests, among others, is to prove that the aircraft is capable of exceeding the number take-off and landing cycles established by the manufacturer. For this purpose, analytical and computer calculations of the airframe structure fatigue life were performed [5]. The results required verification with a full-scale fatigue test of the Su-22 aircraft. This test required full understanding of the external loads applied to the aircraft.

The following presents the method for evaluating the load magnitude acting on the Su-22 flaps. The flaps are structural components mainly operated during the take-off and landing stages of flight. The Su-22 has four flaps (with two on each wing side). The inner flaps are operated during take-off and landing. The outer flaps are used for landing only.

Aircraft flaps are flight safety critical components. Any failure of a flap may have catastrophic consequences. The extreme loads acting on the flaps during take-off and landing increase the relative damage exposure of these components. Fig. 2 shows damage to a Su-22 flap caused by a faulty repair replacement of rivets [2].

Four analytical methods were applied in the flap load estimation to increase the calculation reliability. These include three methods explained in [3, 6, 9] and a method applied in the *Advanced Aircraft Analysis* [1], which is identical to the method in [6]. The methods facilitate calculation of the global loads of the wing with the flaps extended. It was then necessary to estimate what part of those loads is limited to the surface area of the flaps. This required an analysis of the pressure distribution across the airfoils with extended flaps. The XFOIL software [8] was used as being capable of determining the distribution.

The calculation results will be an input to a full-scale fatigue life test of the Su-22 and loading the flaps of the tested aircraft. The test results will help estimate the viability of a safe service life extension for the Su-22 fleet.

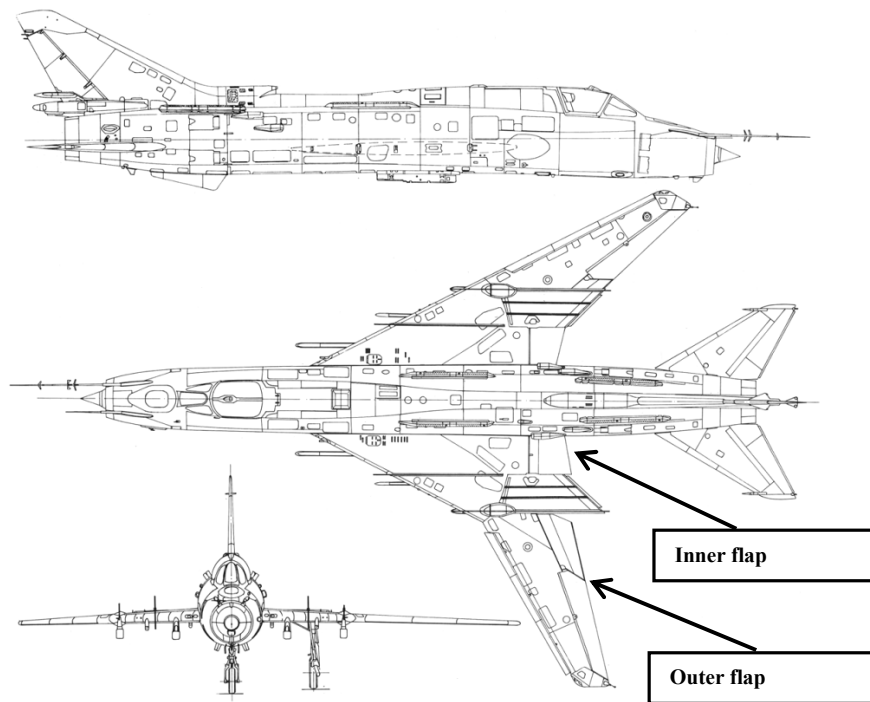


Fig. 1. Diagram of the Su-22 structure



Fig. 2. Damage to a Su-22 flap

2. IDENTIFICATION OF THE AIRCRAFT GEOMETRY

To determine the loads acting on the Su-22 flaps, the aircraft geometry was reproduced from the overview in [7], see Fig. 1. A series of measurements were taken to determine the geometrical features of the fuselage, the wings, the tailplane and the vertical tail units. The aircraft dimension resulting from these calculations were then used to calculate a number of geometrical characteristics of the structural components. These calculations were completed in the AAA3.2 software [1]. Fig. 3 shows the reconstructed geometry of the aircraft and its wing, complete with the outer flap. A series of measurements were also taken directly on the actual Su-22 aircraft to determine, among others, the wing and flap geometrical sections (Figs. 4 and 5).

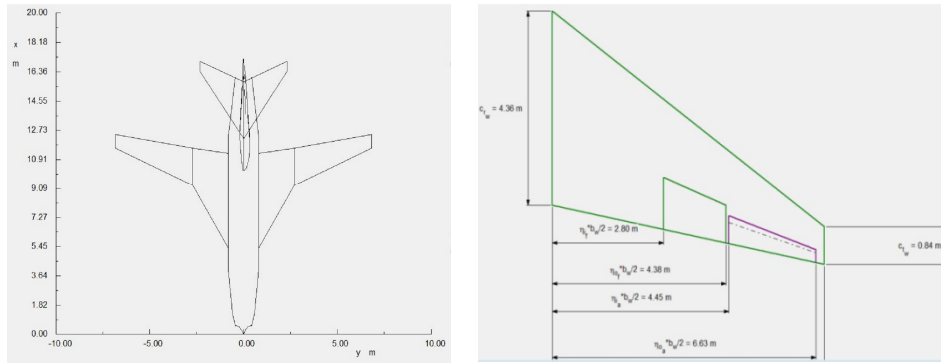


Fig. 3. Reconstructed geometry of the aircraft and its wing, complete with the outer flap

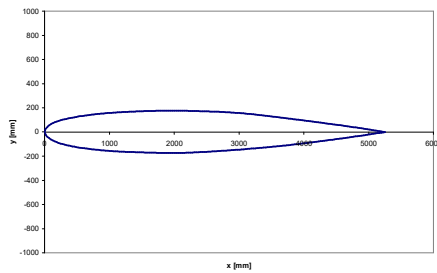


Fig. 4. Wing section in the inner flap vicinity

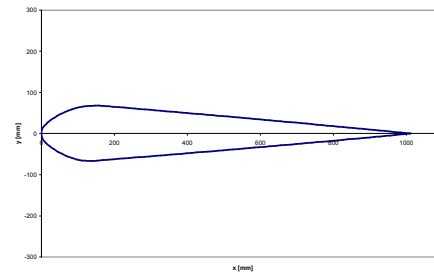


Fig. 5. Inner flap section

3. IDENTIFICATION OF THE CALCULATION METHODS

The following section presents the calculation methods available in the reference literature which enable the effect of flap extension on the increase in the wing lift. These are theoretical and experimental methods which require plotting a large number of charts. The charts contain a number of designations applicable to the wing and flap geometries and may vary with source. Given this problem, this paper uses the original designations. The charts were digitized to help determine the polynomials to approximate the individual curves. The polynomials were applied to determine the values of the coefficients present in the calculation formulas.

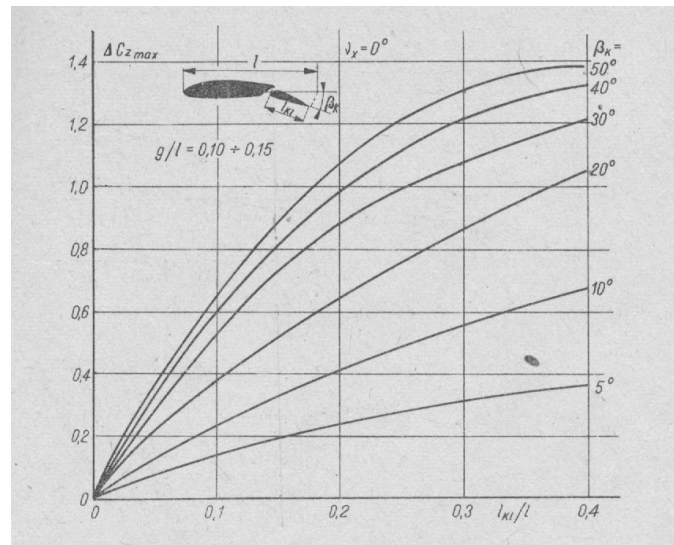
3.1. The Fiszdon calculation method

The monograph [3] shows the charts which enable determining the increase of the lift coefficient for a wing with a slotted flap and a Fowler flap, see Fig. 6. The charts refer to wings with a full wing span flap, which is a two-dimensional case.

The following formula is applied to include the effect of the wing envelope and the flap reach on the increase of the lift coefficient in an actual wing:

$$\Delta C_z = (\Delta C_z)_{2D} \left\{ k_{1z} \left[1 + k_{2z}(A-6) + k_{3z} \sin \nu_{x1/4} \right] - k_{1w} \left[1 + k_{2w}(A-6) + k_{3w} \sin \nu_{x1/4} \right] \right\} \quad (1)$$

(a)



(b)

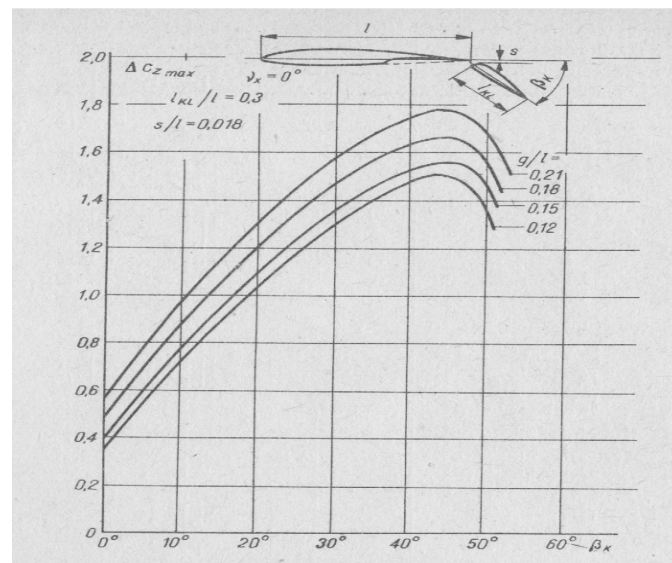


Fig. 6. Increase of the lift coefficient for a slotted flap and a Fowler flap [3]

The factors (k_{1z}, k_{2z}, k_{3z}) and (k_{1w}, k_{2w}, k_{3w}) are determined from Fig. 7 by assuming the following: $\lambda = l_{kl} / l_0$ and $\eta = b_{kz} / b$ for the factors (k_{1z}, k_{2z}, k_{3z}) , or $\eta = b_{kw} / b$ for the factors (k_{1w}, k_{2w}, k_{3w}) . The dimensions l_{kl} , l , b , b_{kw} , b_{kz} are shown in Figs. 6 and 7; A is the aspect ratio; $\nu_{x1/4}$ is the sweep angle of $1/4$ of the chords.

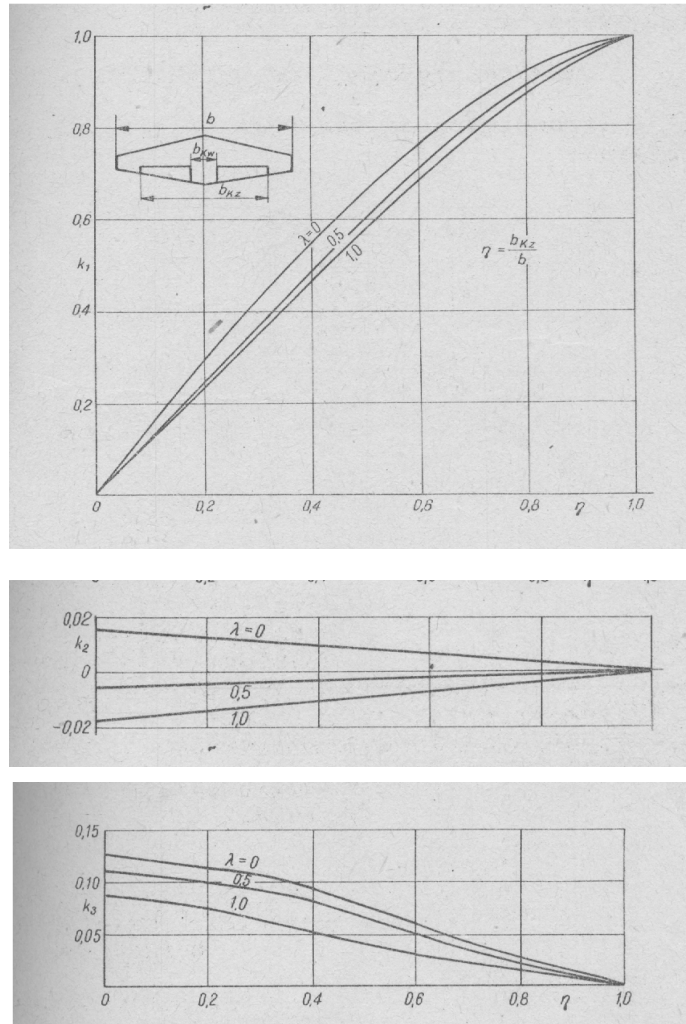


Fig. 7 Correction factors k_1, k_2, k_3 [3]

3.2. The Young calculation method

The publication [9] depicts a method for calculating the increase of the lift coefficient for a wing from the extension of flaps. The method considers the flap angle, the chord change, and the flap range along the wing span.

With the flaps pulled in, the wing chord is c (Fig. 8). Extending of the flap changes the wing chord to a dimension larger or smaller than the chord of the wing with the flap pulled in, which depends on the mechanization of the flap. Hence the so-called effective chord c' is defined.

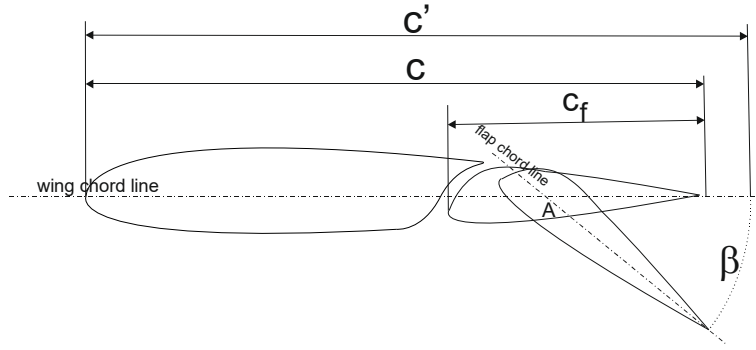


Fig. 8. Diagram of a wing geometry with a flap

The change of the chord and an extension of a full wing span flap increase the lift by:

$$\Delta C_L = \Delta C'_L \frac{c'}{c} \frac{F(A)}{F(6)} + C_{Lw} \left(\frac{c'}{c} - 1 \right) \quad (2)$$

- $F(A)/F(6)$ is a correction factor including the change in the lift curve slope from the change in the aspect ratio relative to the dimensioning aspect ratio $A = 6$. The correction factor is shown in Fig. 9.
- C_{Lw} is the lift coefficient value with the flap pulled in.
- $\Delta C'_L$ is the increment of the lift coefficient calculated with the effective chord included. It is calculated with the expression:

$$\Delta C'_L = \lambda_1 \left(\frac{c_f}{c'} \right) \cdot \lambda_2(\beta) \quad (3)$$

- $\lambda_1 \left(\frac{c_f}{c'} \right)$ – the correction factor dependent on the flap chord c_f to effective chord ratio. It is shown in Fig. 10.
- $\lambda_2(\beta)$ – the correction factor dependent on the flap angle β . It is shown in Fig. 11.

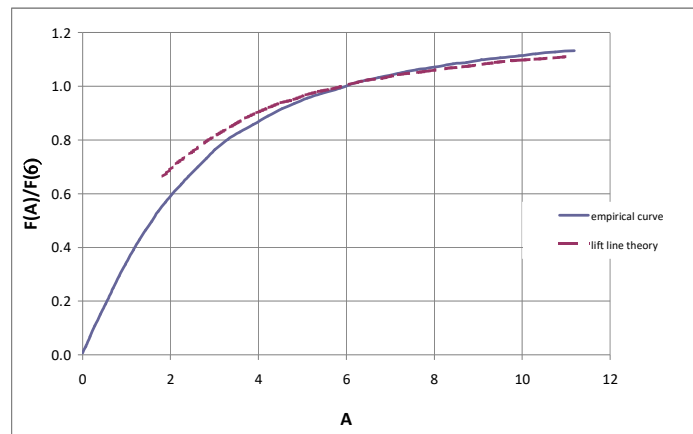


Fig. 9. Correction factor $F(A)/F(6)$

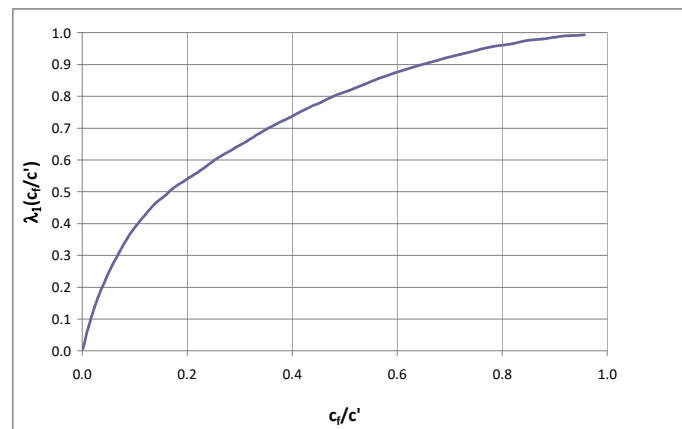
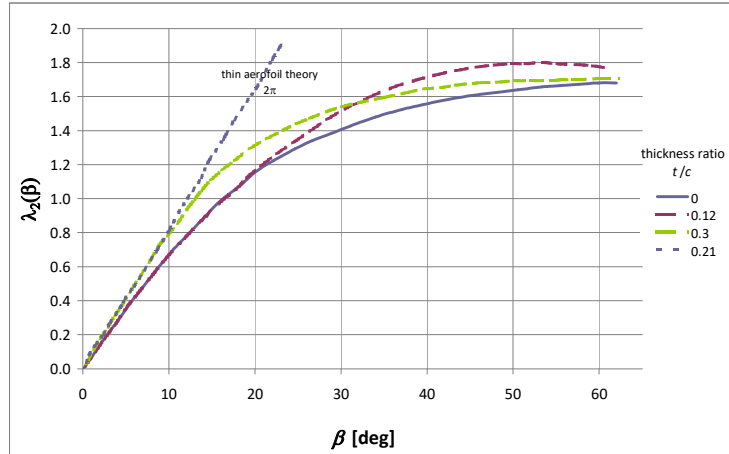
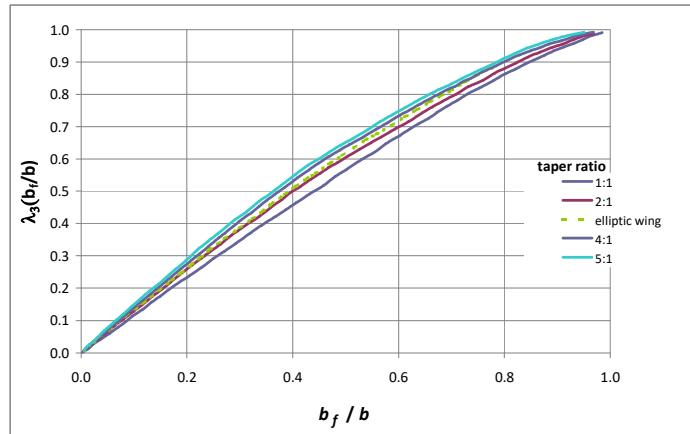


Fig. 10. Correction factor λ_l

Fig. 11. Correction factor λ_2 Fig. 12. Correction factor λ_3

The flap range is included with the following expression:

$$\Delta C_{L_wing} = \Delta C_L \cdot \left[\lambda_3 \left(\frac{b_{fo}}{b} \right) - \lambda_3 \left(\frac{b_{fi}}{b} \right) \right] \quad (4)$$

The factor $\lambda_3 \left(\frac{b_f}{b} \right)$ is shown in Fig. 12. b_{fo} – outer flap edge span; b_{fi} – inner flap edge span.

3.3. The Roskam calculation method

The study [6] depicts a method for calculating the increment of the lift coefficient for a wing from the extension of flaps. This method is the most accurate of those listed herein and considers a large number of factors which determine the performance of flaps.

The flap angle δ_f results in a change of the airfoil lift coefficient:

$$\Delta C_{za_prof} = C_{za_prof}^\alpha \cdot a_\delta \cdot \frac{c'}{c} \cdot \delta_f \tag{5}$$

$C_{za_prof}^\alpha$ – the lift curve slope of the airfoil section with the flaps pulled in and within the small Mach numbers ($M \approx 0$) between 5.44 and 6.7.

c', c – the chords shown in Fig. 8.

a_δ – the flap efficiency factor shown in Fig. 13.

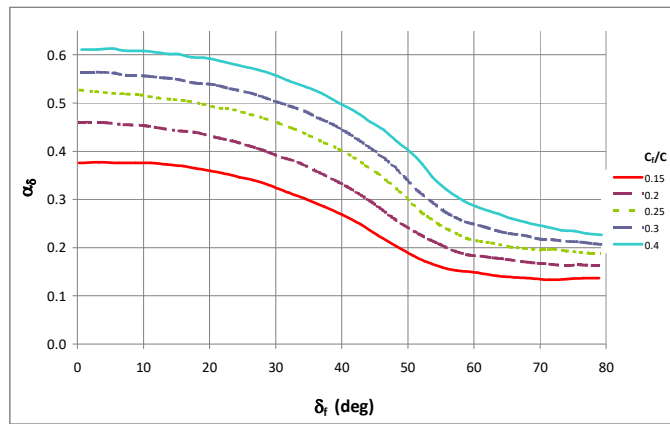


Fig. 13. Flap efficiency factor α_δ

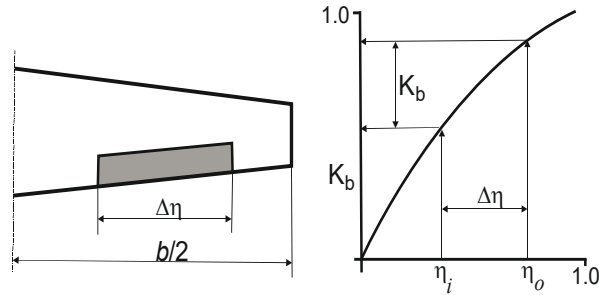


Fig. 14. Diagram for the determination of factor K_b

The lift coefficient change for the whole wing is calculated with this relationship:

$$\Delta C_{za} = \Delta C_{za_prof} \cdot K_b \cdot \frac{(a_\delta)_{C_L}}{(a_\delta)_{C_l}} \cdot \frac{C_{za_wing}^\alpha}{C_{za_prof}^\alpha} \quad (6)$$

where:

ΔC_{za_prof} – the change in the section lift coefficient, expressed by the formula (5).

K_b – the factor dependent on the flap span and the wing taper ratio, determined from Figs. 14 and 15.

$\frac{(a_\delta)_{C_L}}{(a_\delta)_{C_l}}$ – the 3-dimensional flap efficiency factor read from Figs. 16 and 17.

$C_{za_wing}^\alpha$ – the wing lift curve slope calculated with the formula:

$$C_{za_wing}^\alpha = \frac{2\pi A}{2 + \sqrt{\frac{A^2 \beta^2}{k^2} \left(1 + \frac{\tan^2 \Lambda_{c/2}}{\beta^2}\right) + 4}} \quad (7)$$

where:

$A = \frac{b^2}{S}$ – wing aspect ratio

$\Lambda_{c/2}$ – angle of the line of $1/2$ chords

$\beta = \sqrt{1 - M^2}$ – correction factor from the Mach number M

$C_{za_prof_M}^\alpha = \frac{C_{za_prof_M=0}^\alpha}{\beta}$ – section lift curve slope at the Mach number M

$k = \frac{C_{za_prof_M}^\alpha}{2\pi}$ – section lift curve slope at the Mach number M referenced to 2π

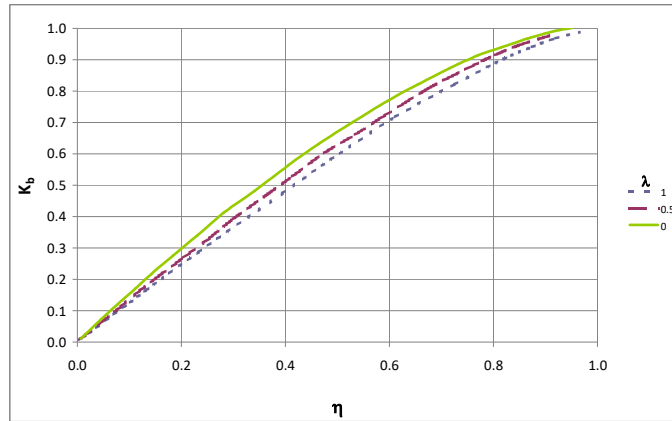


Fig. 15. Coefficient K_b

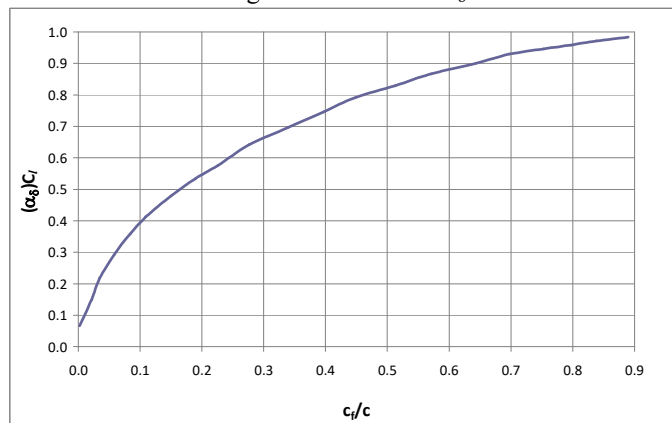


Fig. 16. 3-dimensional flap efficiency factor

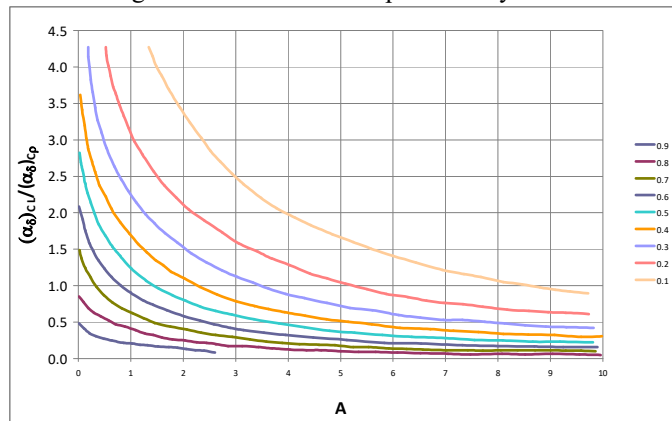


Fig. 17. 3-dimensional flap efficiency factor

4. RESULTS OF CALCULATION FOR FLAPS FROM THE FISZDON, YOUNG AND ROSKAM METHODS

The following section outlines the calculation results for the inner and outer flaps depicted in Fig. 1. The results apply to three of the four analytical methods contemplated herein. The flap angle is 25° for the outer and inner flaps.

4.1. The Fiszdon method

The following table shows the calculation results for the inner and outer flaps. Concerning the inner flap, it was established that Fig. 6(b) applies to a Fowler flap with the wing section relative thickness of $g/l = 12\%$, 15% , 18% , and 21% . The aircraft wing section is 7% in thickness ratio, so the values $(\Delta C_z)_{2D}$ were read at a flap angle of 25° and extrapolated for this thickness ratio. Note that Fig. 6(b) concerns a flap which occupies 30% of the chord, $\lambda = 0.3$, and the calculated value is 0.2 . A respective adjustment was then made to the calculations.

Wing		
Aspect ratio A	$A=5.27$	
Sweep angle of $1/4$ of the chords $V_{x1/4}$	$V_{x1/4} = 30.4^\circ$	
Description	Inner flap	Outer flap
Flap occupancy of the wing section (from Fig. 1 and as measured)	$\lambda = l_{kl}/l = 0.2$	$\lambda = l_{kl}/l = 0.3$
Relative position of flap ends (from Fig. 1 and as measured)	$\eta_{kw} = b_{kw}/b = 0.117$ $\eta_{kz} = b_{kz}/b = 0.257$	$\eta_{kw} = b_{kw}/b = 0.36$ $\eta_{kz} = b_{kz}/b = 0.61$
Auxiliary factors (from Fig. 7)	$k_{1z}=0.367, k_{2z}=0.0764,$ $k_{3z}=0.119, k_{1w}=0.172,$ $k_{2w}=0.00691, k_{3w}=0.111$	$k_{1w}=0.481, k_{2w}=0.0055,$ $k_{3w}=0.1; k_{1z}=0.761,$ $k_{2z}=0.004, k_{3z}=0.058$
Increment of the lift coefficient at the wing section thickness ratio of 7% and $\lambda = 0.3$	$(\Delta C_z)_{2D} = 0.99$	$(\Delta C_z)_{2D} = 0.69$
Increment of the lift coefficient at the wing section thickness ratio of 7% and $\lambda = 0.2$	$(\Delta C_z)_{2D} = 0.99 \cdot \frac{2}{3} = 0.66$	-
Increment of the wing lift coefficient (formula (1))	$\Delta C_z = 0.66 \cdot 0.206 = 0.136$	$\Delta C_z = 0.69 \cdot 0.277 = 0.191$

4.2. The Young method

Description	Inner flap	Outer flap
Increment in chord (as measured)	$c'/c = 1.04$	$c'/c = 1.0$
Change of the lift curve slope at the aspect ratio $A=5.27$ (Fig. 9)	$F(A)/F(6) = 0.95$	
Correction factor (Fig. 10)	$c_f/c' = 0.2 \rightarrow \lambda_1 = 0.55$	$c_f/c' = 0.3 \rightarrow \lambda_1 = 0.64$
Correction factor for the flap angle $\beta = 25$ (Fig. 11)	$\lambda_2 = 1.34$	
Increment of the wing lift coeff. with the effective chord (formula (3))	$\Delta C'_L = \lambda_1 \cdot \lambda_2 = 0.737$	$\Delta C'_L = \lambda_1 \cdot \lambda_2 = 0.857$
Increment of the wing lift coeff. with the effective chord for the full wing span flap (formula (2))	$\Delta C_L = \Delta C'_L \frac{c'}{c} \frac{F(A)}{F(6)} = 0.728$	$\Delta C_L = \Delta C'_L \frac{c'}{c} \frac{F(A)}{F(6)} = 0.814$
Factors with the flap range (Fig. 12)	$\frac{b_{fi}}{b} = 0.117 \rightarrow \lambda_3 \left(\frac{b_{fi}}{b} \right) = 0.172$ $\frac{b_{fo}}{b} = 0.257 \rightarrow \lambda_3 \left(\frac{b_{fo}}{b} \right) = 0.367$	$\frac{b_{fi}}{b} = 0.36 \rightarrow \lambda_3 \left(\frac{b_{fi}}{b} \right) = 0.488$ $\frac{b_{fo}}{b} = 0.61 \rightarrow \lambda_3 \left(\frac{b_{fo}}{b} \right) = 0.76$
Increment of the wing lift coeff. with the flap range (formula (4))	$\Delta C_{L_wing} = 0.142$	$\Delta C_{L_wing} = 0.221$

4.3. The Roskam method

Due to the missing data for the wing section, the calculation was performed with two limit values $C_{za_prof}^{\alpha}$ shown below. The Mach number was considered with two cases: - the flap pull-in speed of 450 km/h (125 m/s) and the maximum permitted speed with the flaps extended 600 km/h (166 m/s). The correction factor values are $\beta = 0.93$ and $\beta = 0.87$, respectively. A mean value $\beta = 0.9$ was used for this calculation.

Description	Inner flap	Outer flap
Increment in chord (as measured)	$c'/c = 1.04$	$c'/c = 1.0$
Wing section lift characteristic gradient (from [6])	$C_{za_prof}^\alpha = \begin{pmatrix} 5.44 \\ 6.7 \end{pmatrix}$	
Flap efficiency factor (Fig. 13)	$\delta_f = 25^\circ, c_f/c' = 0.2$ $\rightarrow a_\delta = 0.413$	$\delta_f = 25^\circ, c_f/c' = 0.3$ $\rightarrow a_\delta = 0.52$
Increment of the wing section lift coefficient (formula (5))	$\Delta C_{za_prof} = \begin{pmatrix} 1.032 \\ 1.27 \end{pmatrix}$	$\Delta C_{za_prof} = \begin{pmatrix} 1.234 \\ 1.52 \end{pmatrix}$
Correction factor from the Mach number	$\beta = 0.9$	
Wing section lift curve slope with the Mach number	$C_{za_prof_M}^\alpha = \frac{\begin{pmatrix} 5.44 \\ 6.7 \end{pmatrix}}{0.9} = \begin{pmatrix} 6.04 \\ 7.44 \end{pmatrix}$	
Wing section relative characteristic gradient $C_{za}(\alpha)$ at the Mach number M	$k = \frac{\begin{pmatrix} 6.04 \\ 7.44 \end{pmatrix}}{2\pi} = \begin{pmatrix} 0.96 \\ 1.18 \end{pmatrix}$	
Wing lift curve slope (formula (7))	$A = 5.27, \Lambda_{c/2} = 23^\circ \rightarrow C_{za_wing}^\alpha = \begin{pmatrix} 4.22 \\ 4.80 \end{pmatrix}$	
Factor dependent on the flap span and the wing taper (Figs. 14 and 15)	$\eta_i = 0.117, \eta_o = 0.257$ $\rightarrow K_b = 0.195$	$\eta_i = 0.36, \eta_o = 0.61$ $\rightarrow K_b = 0.19$
3-dimensional flap efficiency factor (Figs. 14 and 15)	$\frac{(a_\delta)_{C_L}}{(a_\delta)_{C_i}} = 1.069$	$\frac{(a_\delta)_{C_L}}{(a_\delta)_{C_i}} = 1.05$
Change of the full wing lift coefficient (formula (6))	$\Delta C_{za} = \begin{pmatrix} 0.167 \\ 0.183 \end{pmatrix}$	$\Delta C_{za} = \begin{pmatrix} 0.172 \\ 0.196 \end{pmatrix}$

4.4. Advanced Aircraft Analysis method [2]

Based on the inputs provided, the AAA3.2 software can calculate the value of the increase in the lift coefficient from the extension of the flaps. Fig. 18 shows a parameter table filled with the data for the inner flaps (see the blue frame). The table also states the calculated values of the increase in the lift coefficient for an angle of attack which corresponds to zero lift (i.e. the wing with the flaps pulled in) and an angle of attack which corresponds to the maximum lift (see the red frames).

These values are equal to $\Delta C_{za} = \begin{pmatrix} 0.1679 \\ 0.1862 \end{pmatrix}$. The outer flap generated the values $\Delta C_{za} = \begin{pmatrix} 0.2763 \\ 0.3131 \end{pmatrix}$.

Parameter	Value	Unit
Altitude	10000	m
ΔT	0.0	deg C
U_1	360.00	km/hr
AR_w	5.27	
λ_w	0.19	
M_1	0.334	
$\Delta c_{l,max} / \Delta c_{l1}$	0.9542	
α_{1y}	0.4108	
α_{cfl_w}	30.0	deg
α_1	11.7	%
α_2	25.7	%
c_l/c_w	20.0	%
δ_1	25.0	deg
ΔC_{z_a}	0.1862	
ΔC_{z_a}	0.1679	

Fig. 18. Table of calculation parameters for the inner flap

4.5. Summary of the calculations of ΔC_{za} for the flaps

The individual methods provided different yet approximate values of the increase in the wing lift coefficient caused by a flap angle of 25°. These values served to calculate the mean values as the inputs for downstream calculations. This is shown in Table 1.

Table 1. Calculated lift coefficient increase values

Method	Inner flap	Outer flap
Fiszdon	$\Delta C_{za}=0.136$	$\Delta C_{za}=0.191$
Young	$\Delta C_{za}=0.142$	$\Delta C_{za}=0.221$
Roskam	$\Delta C_{za} = \begin{pmatrix} 0.167 \\ 0.183 \end{pmatrix}$	$\Delta C_{za} = \begin{pmatrix} 0.172 \\ 0.196 \end{pmatrix}$
AAA3.2	$\Delta C_{za} = \begin{pmatrix} 0.1679 \\ 0.1862 \end{pmatrix}$	$\Delta C_{za} = \begin{pmatrix} 0.2763 \\ 0.3131 \end{pmatrix}$
Mean value	$\Delta C_{za}=0.163$	$\Delta C_{za}=0.228$

5. ANALYSIS OF THE SU-22 WING SECTION CHARACTERISTICS

The Su-22 aircraft technical documentation does not specify the wing section. The only available data states a relative section thickness of 7%.

In order to determine the approximate characteristics of the wing section, measurements of the actual Su-22 wing section (see Fig. 4) were used. The wing section is biconvex with a calculated thickness ratio of 6.652% and the maximum centre line camber of 0.1%. The coordinates of the wing section points were input to the XFOIL software. Once standardised, the inputs served to calculate the aerodynamic characteristics, where pressure distribution across the wing section and the characteristic $C_{za}(\alpha)$ were calculated for a number of different angles of attack. They are shown in Figs. 19 and 20. The characteristic $C_{za}(\alpha)$ facilitates calculation of this derivative: $C_{za_prof}^{\alpha} = 6.59$. The value is within the interval estimated in Section 4.3.

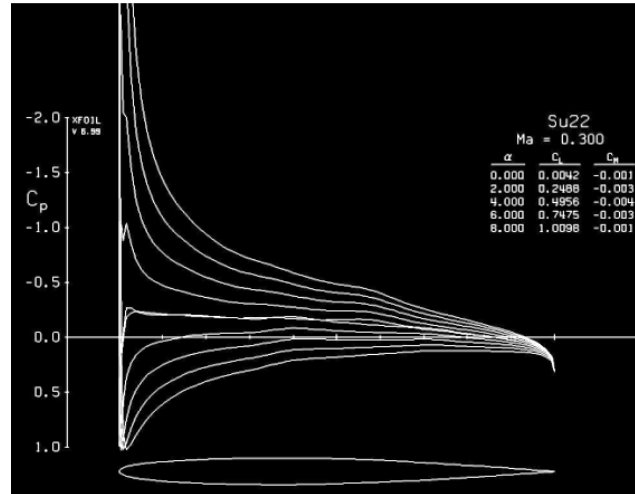


Fig. 19. Pressure distribution across a Su-22 wing section at various angles of attack

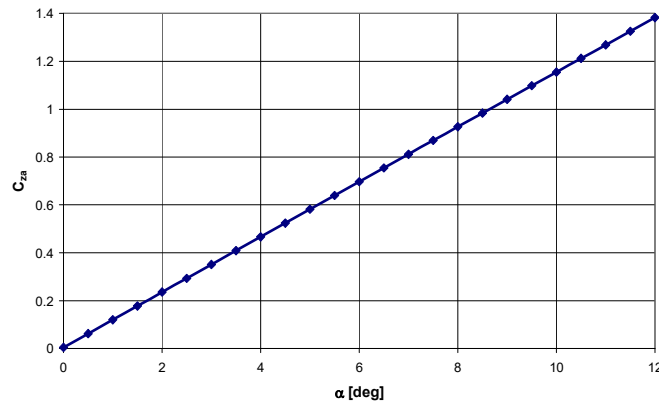


Fig. 20. Characteristic $C_{za}(\alpha)$ of a Su-22 wing section

6. VERIFICATION OF THE CALCULATIONS BY CROSS-REFERENCE WITH THE AIRCRAFT MANUALS

The [7] shows the aircraft characteristic $C_{za}(\alpha)$ at a sweep angle of 30° without considering a mechanization of the flaps, see Fig. 21 (solid line: no slots; dashed line: 10° slots).[7] also shows the polar curve of the aircraft and the characteristic $C_{za}(\alpha)$ at a sweep angle of 30° with the ground effect in three configurations: 1 – (10° slots; all flaps pulled in); 2 – (10° slots; inner flaps at 25° ; outer flaps pulled in); 3 – (10° slots; inner flaps at 25° ; outer flaps at 25°). It is shown in Fig. 22.

The two figures help estimate the effect of the flap angle on the changes of the lift coefficient. Table 2 shows the lift coefficient increase values read from references and theoretically calculated in prior. The theoretical values are higher than the reference readings. The increase values grow as the angle of attack is reduced. Fig. 21 shows that the increase of the lift coefficient after extending the outer flaps is between 0.2 and 0.1, depending on the angle of attack. The increase at small angles of attack is approximate to the calculated value of 0.228. With the small angles of attack applied to high flight speeds, it can be assumed that the flap extension/pull-in speed (450 km/h) requires higher values.

This analysis also permits a conclusion that the calculated values of the increase ΔC_{za} assumed to determine the flap load force values will result in flap load tests under conditions that will be more extreme than in normal flight operations. This means that a positive result of load tests will guarantee proper performance of the flaps in further service of the aircraft.

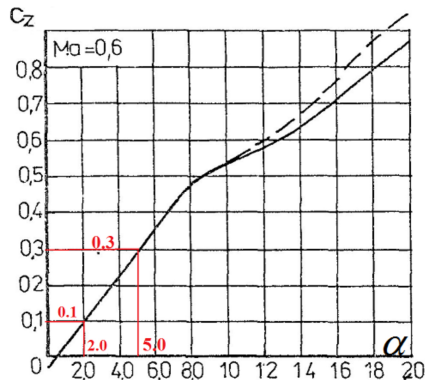


Fig. 21. Characteristic $C_{za}(\alpha)$ [7]

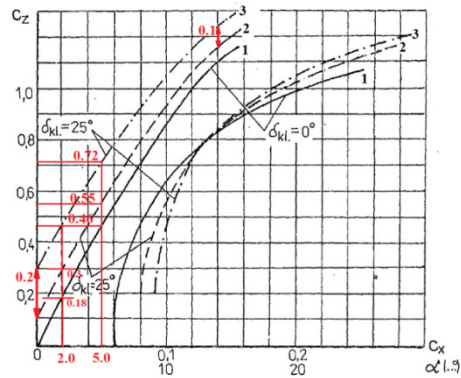


Fig. 22. Aircraft polar curve and $C_{za}(\alpha)$ [7]

Table 2. Lift coefficient increase values

Item	Configuration	$\alpha = 2^\circ$	$\alpha = 5^\circ$	Calculations
1	Effect of 10° slot angle	0.08	0.16	-
2	Effect of 25° inner flap angle	0.12	0.09	0.164
3	Effect of 25° outer flap angle	0.16	0.17	0.228

7. VERIFICATION OF THE CALCULATIONS OF WIND SECTION LIFT COEFFICIENT INCREASE

The XFOIL software was applied to calculate the increase in the lift coefficient of the Su-22 wing (Fig. 23) from a flap angle of 25° . The angle of attack was $\alpha = 0^\circ$. The calculations included the influence of Mach numbers and the Reynolds numbers. Both numbers were determined for a calculated speed of 450 km/h (125 m/s) and a mean aerodynamic chord $b_a = 2.99$ m.

The results: $Ma = 0.36$, $Re = 26 \cdot 10^6$. Fig. 23 shows the examples of calculations of the wing section with a flap extended and occupying 30% of the chord. The obtained lift coefficient increase values were compared to the previous results, see Table 3. The comparison shows that, in the case of the inner flap, the values calculated with the XFOIL, Fiszdon and Roskam methods are approximate. As for the outer flap, the values from the XFOIL and Roskam methods are similar.

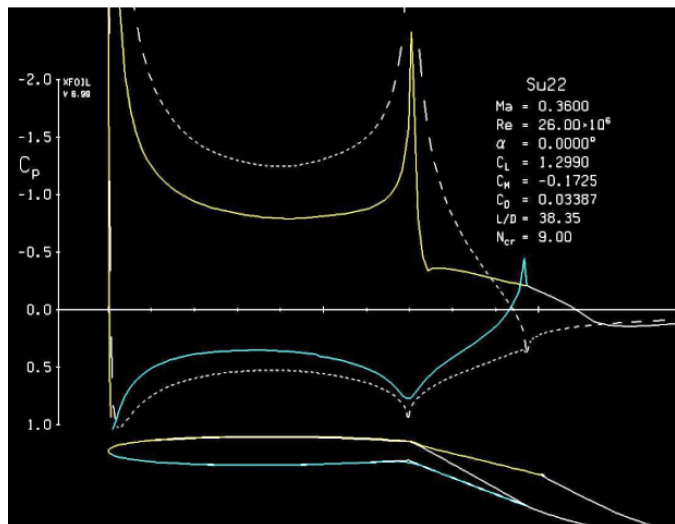


Fig. 23. Airflow of the Su-22 section with a flap extended and occupying 30% of the chord

Table 3. Lift coefficient of the Su-22 wing section (2D case)

Calculation method	Flap at 20% (inner)	Flap at 30% (outer)
XFOIL	1.087	1.296
Fiszdon	0.99	0.69
Young	0.737	0.857
Roskam	$\begin{pmatrix} 1.032 \\ 1.27 \end{pmatrix}$	$\begin{pmatrix} 1.234 \\ 1.52 \end{pmatrix}$

8. CALCULATION OF THE FLAP LOADING FORCES

The inner flap is operated both during take-off and landing. The outer flap is intended for aircraft landing only. This means that the take-off stage is dimensioning for the inner flap and the landing stage is dimensioning for the outer flap.

8.1. Calculation of the inner flap loading force during take-off

Fig. 24 shows a diagram of the forces acting on the aircraft during climb. It shows that the aircraft lift is $P_{za} \approx Q/\cos\gamma_a$. The coefficient C_{za} can be calculated:

$$C_{za} = \frac{1}{\cos\gamma_a} \frac{2mg}{\rho V^2 S} \quad (8)$$

This is a lift coefficient with the inner flaps extended. Its value is equal to the sum of the lift coefficient of the wing with the flaps pulled in, $C_{za_{\delta_f=0}}$ and the previously calculated increase values for the inner flaps, $\Delta C_{za_{inner}}$.

$$C_{za} = C_{za_{\delta_f=0}} + \Delta C_{za_{inner}} \quad (9)$$

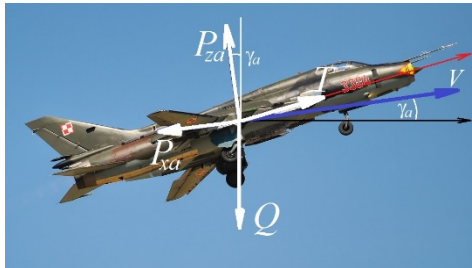


Fig. 24. Diagram of the force distribution during climb

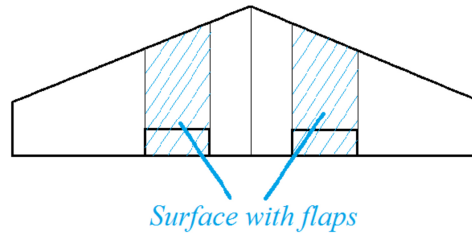


Fig. 25. Determination of the wing surface occupied by the flaps

Hence the total lift can be expressed as follows:

$$P_{za} = P_{za_{\delta_f=0}} + \Delta P_{za_inner} \quad (10)$$

The individual components are equal to, respectively:

$$P_{za_{\delta_f=0}} = C_{za_{\delta_f=0}} \frac{\rho V^2}{2} S, \quad \Delta P_{za_inner} = \Delta C_{za_inner} \frac{\rho V^2}{2} S \quad (11)$$

The lift $P_{za_{\delta_f=0}}$ is generated over the entire wing area, whereas the lift ΔP_{za_inner} applies only to the wing areas occupied by the flaps (Fig. 25). Given that the force distribution $P_{za_{\delta_f=0}}$ along the wing is proportional to the wing surface area and that the force from the inner flap extension ΔP_{za_inner} applies only to the wing areas occupied by the inner flaps, it is possible to calculate the total forces generated within the wing areas occupied by the inner flaps:

$$P_{za_inner} = P_{za_{\delta_f=0}} \frac{S_{p_z_k_w}}{S} + \Delta P_{za_inner} = \left(C_{za_{\delta_f=0}} S_{p_z_k_w} + \Delta C_{za_inner} S \right) \frac{\rho V^2}{2} \quad (12)$$

The following values were established from the aircraft drawings and technical manuals: – reference area $S = 35.54 \text{ m}^2$; – wing area occupied by the inner flaps $S_{p_z_k_w} = 9.44 \text{ m}^2$; – maximum take-off weight of the aircraft $m = 19400 \text{ kg}$; – take-off speed $V = 360 \div 365 \text{ km/h}$ ($100 \div 101.4 \text{ m/s}$); – flap pull-in speed $V = 420 \div 450 \text{ km/h}$ ($116.7 \div 125 \text{ m/s}$). The assumed increase value of the lift coefficient for the inner flap $\Delta C_{za} = 0.164$.

Because the references specify that the take-off pitch is 10° ($15^\circ \div 20^\circ$ during an afterburner take-off), calculations were performed for three different flight path angles, $\gamma_a = 0^\circ, 20^\circ, \text{ and } 30^\circ$. The resulting values of the lift coefficient C_{za} (formula (9)) and $C_{za_{\delta_f=0}}$ and the force P_{za_inner} are shown in Table 4.

Table 4. Forces within the wing areas occupied by two inner flaps

Climb angle γ_a	C_{za}	$C_{za_{\delta_f=0}}$	P_{za_inner} [N]
0°	0.85	0.686	77 529
20°	0.904	0.74	80 774
30°	0.981	0.817	85 351

The results allowed a conclusion that the highest load force acting on the wing area occupied by a single inner flap is 42676 N. This load is applied at a climb at 30° and corresponds to the value $C_{za_{\delta_f=0}} = 0.817$. According to Fig. 21 (dashed line), this value is valid for an angle of attack of 17° .

The distribution of the calculated loading force (across the wing area occupied by the flaps) results directly from the pressure distribution along the chord of the top and bottom surfaces of the wing. These distributions must be identified to calculate what part of the force acts on the flaps. They were established with suitable calculations in the XFOIL software for several angle of attack values. The value of 17° was not achieved due to the inherent constraints of the software. The pressure distributions were approximate to those shown in Fig. 23. The total surface area between the top and bottom curve for the entire section, S_p and the flap-occupied area, S_k were determined with the pressure distributions. The inner flap loading force was calculated with the expression:

$$P_{za_flap_inner} = \frac{P_{za_inner}}{2} \frac{S_k}{S_p} \quad (13)$$

with the measured values $S_p=1.478$ and $S_k=0.186$ the resulting value $P_{za_flap_inner} = 5400$ N. This is the dimensioning force which loads the inner flap during take-off.

8.2. Calculation of the loading forces of the inner and outer flaps during landing

Similar to the take-off and climb, the relationship between the lift of steady descent and the aircraft weight is (8). Now the required lift coefficient can be calculated, see formula (9). In the case of the landing stage, this is the lift coefficient with both inner and outer flaps extended. Its value is equal to the lift coefficient of the wing with the flaps pulled in, $C_{za_δ_f=0}$ and the previously calculated increase values for the inner flaps, ΔC_{za_inner} and the outer flaps, ΔC_{za_outer} :

$$C_{za} = C_{za_δ_f=0} + \Delta C_{za_inner} + \Delta C_{za_outer} \quad (14)$$

Hence the total lift can be expressed as follows:

$$P_{za} = P_{za_δ_f=0} + \Delta P_{za_inner} + \Delta P_{za_outer} \quad (15)$$

By applying the calculations analogous to those in Section 8.1, expressions are derived which determine the flap loading forces during landing:

$$\begin{aligned}
 P_{za_inner} &= \left(C_{za_{\delta_f=0}} S_{p_z_k_w} + \Delta C_{za_inner} S \right) \frac{\rho V^2}{2}, \\
 P_{za_outer} &= \left(C_{za_{\delta_f=0}} S_{p_z_k_z} + \Delta C_{za_outer} S \right) \frac{\rho V^2}{2}
 \end{aligned} \quad (16)$$

Further calculations included the previously stated values of the reference area and the inner flap surface area with:

- the wing surface occupied by the outer flaps, $S_{p_z_k_z} = 6.38 \text{ m}^2$;
- the maximum permitted landing mass of the aircraft $m = 13400 \text{ kg}$;
- the landing speed $V = 285 \div 300 \text{ km/h}$;
- the lift coefficient increase values

$$\Delta C_{za_inner} = 0.164 ; \Delta C_{za_outer} = 0.228 .$$

The references specify that the landing pitch is -10° , calculations were performed for three different flight path angles, $\gamma_a = 0^\circ, -10^\circ, \text{ and } -20^\circ$. The resulting values of the lift coefficient C_{za} (formula (9)) and $C_{za_{\delta_f=0}}$ and the force P_{za_inner} and P_{za_outer} are shown in Tables 5 and 6.

Table 5. Forces in the areas occupied by two flaps at the landing speed of 285 km/h

Flight path angle γ_a	C_{za}	$C_{za_{\delta_f=0}}$	P_{za_inner}	P_{za_outer}
0°	0.963	0.571	43093 N	45123 N
-10°	0.978	0.586	43632 N	45487 N
-20°	1.024	0.632	45334 N	46638 N

Table 6. Forces in the areas occupied by two flaps at the landing speed of 300 km/h

Flight path angle γ_a	C_{za}	$C_{za_{\delta_f=0}}$	P_{za_inner}	P_{za_outer}
0°	0.870	0.478	43968 N	47427 N
-10°	0.883	0.491	44507 N	47791 N
-20°	0.925	0.533	46210 N	48942 N

Based on the results (see Table 6) it was assumed that the highest loading force value of the areas occupied by single flaps is, respectively: 23104 N for the inner flap and 24471 N for the outer flap. The loads are generated when the aircraft is descending at -20° and correspond to $C_{za_{\delta_f=0}} = 0.471$ and an angle of attack $\alpha = 8^\circ$, as established from Fig. 21.

The part of the calculated forces applicable to the flaps was calculated by computing the pressure distributions on the top and bottom areas of the wing profile at this angle of attack in XFOIL.

The total surface area between the top and bottom pressure curve for the entire section, S_p and the flap-occupied area, S_k were determined with the pressure distributions. The flap loading forces were calculated with the expression:

$$P_{za_flap_inner} = \frac{P_{za_inner}}{2} \frac{S_k}{S_p}, \quad P_{za_flap_outer} = \frac{P_{za_outer}}{2} \frac{S_k}{S_p} \quad (17)$$

With the values measured for the inner flap $S_p = 1.478$ and $S_k = 0.186$ the resulting value $P_{za_flap_inner} = 2911$ N. This is the dimensioning force which loads the inner flap during take-off. As for the outer flap, the values measured were $S_p = 1.56$, $S_k = 0.257$, providing the outer flap loading force of $P_{za_flap_outer} = 4035$ N.

9. SUMMARY

Based on the calculations discussed above, the maximum flap loading forces are, respectively:

- $P_{za_flap_inner} = 5400$ N for the inner flap,
- $P_{za_flap_outer} = 4035$ N for the outer flap.

The force identified for the inner flap is applied during take-off, whereas the force identified for the outer flap is applied during landing. These are the force values that should be applied to the respective flaps during the fatigue life test of the aircraft structure.

REFERENCES

- [1] *Advanced Aircraft Analysis ver.3.2.* 2012. DAR Corporation.
- [2] Baraniecki Robert, Marcin Kurdelski, Andrzej Leski 2007. Analiza numeryczna stanu naprężenia w klapie samolotu odrzutowego. *W Materiały X Konferencji nt. Programy MES w Komputerowym Wspomaganiu Analizy, Projektowania i Wytwarzania*, Kazimierz Dolny.
- [3] Fiszdon Władysław. 1961. *Mechanika lotu*. Warszawa, PWN.
- [4] Klimaszewski S., Marcin Kurdelski, Andrzej Leski. 2004. Pomiar sił w elementach struktury samolotu Su-22, *W Materiały VI Konferencji nt. Metody i Technika Badań Powietrznych w Locie*, 235-241. Mrągowo, 15-18 czerwca 2004, Instytut Techniczny Wojsk Lotniczych.
- [5] Kurdelski Marcin, Robert Baraniecki, Andrzej Leski. 2006. „Numeryczne obliczenia trwałości zmęczeniowej głównego węzła mocowania skrzydła samolotu wojskowego”. *Biuletyn WAT LV(4)* : 113-125.
- [6] Roskam Jan. 1987. *Airplane Design – Part 6 Preliminary Calculations of Aerodynamic, Thrust and Power Characteristics*, RAEC.

- [7] *Samolot Su-22UM3K Charakterystyki lotno-techniczne*. 1990. Poznań: Dowództwo Wojsk Powietrznych.
- [8] *XFOIL Subsonic Airfoil Development System*, <http://web.mit.edu/drela/Public/web/xfoil/>
- [9] Young A.D. 1953. *The Aerodynamic Characteristics of Flaps*. Reports of Memoranda no. 2622.

Oszacowanie obciążenia klap samolotu Su-22 na potrzeby prób zmęczeniowych

Grzegorz KOWALECZKO¹, Andrzej LESKI², Wojciech ZIELIŃSKI²

¹ *Wyższa Szkoła Oficerska Sił Powietrznych,
ul. Dywizjonu 303 nr 35, 08-521 Dęblin,*

² *Instytut Techniczny Wojsk Lotniczych,
ul. Księcia Bolesława 6, 01-494 Warszawa*

Streszczenie. W pracy przedstawiono wyniki obliczeń sił działających na kłapy samolotu Su-22 podczas startu i lądowania. Wykorzystano cztery różne analityczno-eksperymentalne metody obliczeniowe w celu zwiększenia wiarygodności otrzymanych rezultatów. Będą one stanowić podstawę do przeprowadzenia prób zmęczeniowych tych elementów konstrukcyjnych skrzydła samolotu. Próby te wykonane będą w ramach szerszego programu badań, mających na celu wydłużenie procesu eksploatacji samolotu Su-22.

Słowa kluczowe: mechanika, badania zmęczeniowe samolotów, obciążenia aerodynamiczne, kłapy samolotu